

18. To explore further whether the differences in listening preferences between the two groups of infants were attributable to prior experience with the stories, the data from the two groups of infants were combined for a 2 (test group) × 2 (list type) analysis of variance. Only the interaction between the test group and list type was significant [$F(1, 28) = 5.60, P < 0.03$], confirming that the preference for the story-word lists occurred only when infants had had prior exposure to the stories.

19. P. D. Eimas and P. C. Quinn, *Child Dev.* **65**, 903 (1994); J. M. Mandler and L. McDonough, *Cogn. Dev.* **8**, 291 (1993); P. C. Quinn, P. D. Eimas, S. L. Rosenkrantz, *Perception* **22**, 463 (1993).
20. R. Baillargeon and J. DeVos, *Child Dev.* **62**, 1227 (1991); E. Spelke, *Cognition* **50**, 431 (1994); K. Breinlinger, J. Macomber, K. Jacobson, *Psychol. Rev.* **99**, 605 (1992).
21. P. Marler, *Dev. Psychobiol.* **23**, 557 (1990).
22. Supported by a research grant from NIH to P.W.J.

(HD15795). We thank A. M. Jusczyk, N. Redanz, D. Dombrowski, B. Boyle, and S. Elsis for their help in recruiting and testing participants and M. Brent, P. Smolensky, G. Ball, R. Tincoff, T. Nazzi, D. Houston, and two anonymous reviewers for helpful comments that they made on early versions of the manuscript. The parents of all infant participants gave informed consent.

22 July 1997; accepted 19 August 1997

LKLF: A Transcriptional Regulator of Single-Positive T Cell Quiescence and Survival

Chay T. Kuo, Margaret L. Veselits, Jeffrey M. Leiden*

Mature single-positive (SP) T lymphocytes enter a "resting" state in which they are proliferatively quiescent and relatively resistant to apoptosis. The molecular mechanisms regulating this quiescent phenotype were unknown. Here it was found that the expression of a Kruppel-like zinc finger transcription factor, lung Kruppel-like factor (LKLF), is developmentally induced during the maturation of SP quiescent T cells and rapidly extinguished after SP T cell activation. LKLF-deficient T cells produced by gene targeting had a spontaneously activated phenotype and died in the spleen and lymph nodes from Fas ligand-induced apoptosis. Thus, LKLF is required to program the quiescent state of SP T cells and to maintain their viability in the peripheral lymphoid organs and blood.

Single-positive (CD4⁺ or CD8⁺) mature T cells circulate through the blood and peripheral lymphoid organs in a quiescent or resting state until they encounter their cognate antigen bound to a major histocompatibility molecule (MHC) on the surface of an appropriate antigen-presenting cell (1). Engagement of the T cell antigen receptor (TCR) by the peptide antigen-MHC complex leads to T cell activation, a process that involves the highly orchestrated expression of more than 100 new genes and concomitant cell cycle progression and proliferation (2). Activated T cells acquire a characteristic set of cell surface markers and are more sensitive to apoptosis (3, 4). Many activated T cells die in the peripheral lymphoid organs from activation-induced cell death, an apoptotic pathway that has been postulated to protect the host against autoimmune disease (5). Several transcription factors, including activation protein-1 (AP1), nuclear factor of activated T cells (NFAT), nuclear factor- κ B (NF- κ B), and the cAMP response element binding protein (CREB), are known to be important positive regulators of activation-specific T cell gene expression (6, 7). However, it was not known if specific transcription factors are also required to program or maintain the quiescent state in resting SP T cells (8).

The erythroid Kruppel-like factor (EKLF)

is an erythroid-specific zinc finger transcription factor that binds to CACCC sequence motifs in the promoter of the β -globin gene and regulates the terminal stages of erythroid development (9). To identify EKLF-related genes that might play a similar role in T cell development, we screened an embryonic mouse cDNA library under low-stringency hybridization conditions with a probe derived from the zinc finger region of EKLF (10). We identified three additional KLF family members, BKLF, GKLF, and LKLF (11). To determine whether any of these other KLF proteins might participate in T cell development, we hybridized Northern (RNA) blots and mouse tissue sections to probes specific for each cDNA. LKLF was expressed in the lung, the vasculature, the heart, skeletal muscle, kidney, and testis as well as in the lymphoid organs of the mouse (Fig. 1A) (12). Within the thymus, LKLF was expressed exclusively in lymphoid cells in the thymic medulla, a region that contains mature SP thymocytes (Fig. 1B). LKLF was also expressed in large amounts in lymphoid cells in the white pulp of the spleen (12). To more precisely characterize LKLF expression in the hematopoietic lineages, we did Northern blot analyses on purified populations of hematopoietic cells (Fig. 1A). LKLF was expressed in both CD4⁺ and CD8⁺ SP thymocytes and splenocytes, but it was undetectable in less mature double-positive (DP) CD4⁺CD8⁺ thymocytes (Fig. 1A). LKLF was also expressed in B220⁺ immunoglobulin M (IgM)-positive splenic B

cells and in bone marrow macrophages (Fig. 1A). LKLF mRNA and protein were decreased significantly after the TCR-mediated activation of quiescent splenic T cells (Fig. 1, C and D). Degradation of the LKLF protein preceded disappearance of the mRNA, suggesting that both LKLF mRNA and protein are regulated after T cell activation. This developmentally and activation-regulated pattern of expression suggested that LKLF might play an important role in regulating the function of resting SP T cells in vivo.

We used homologous recombination in murine embryonic stem (ES) cells to produce a targeted mutation of the *LKLF* gene (Fig. 2A). The resulting null mutation deleted the entire *LKLF* gene. Heterozygous (*LKLF*^{+/-}) mutant ES cell clones produced with a phosphoglycerate kinase-*neomycin* resistance (PGK-*neo*^r) targeting vector (Fig. 2A) were retransfected with a PGK-*hygro*^r targeting vector (Fig. 2A) to produce three independently derived homozygous (*LKLF*^{-/-}) ES cell clones. The genotypes of these clones were confirmed by Southern (DNA) blot analysis (Fig. 2B). Each clone contained single *neo*^r and *hygro*^r integrations. By Northern blot analysis, each of the homozygous clones lacked detectable LKLF mRNA (Fig. 2C).

LKLF^{+/-} ES cell clones were used to produce chimeric mice, which transmitted the targeted allele through the germ line (13). Heterozygous (*LKLF*^{+/-}) mice were phenotypically normal and were bred to produce LKLF-deficient animals. Mice homozygous for the LKLF mutation died between embryonic days 12.5 and 14.5 as a result of intra-amniotic and intra-embryonic hemorrhages (13). To analyze the role of LKLF in lymphoid development and function, we injected three independently derived *LKLF*^{-/-} ES cell clones and two *LKLF*^{+/-} ES cell clones into recombination activating gene 2-deficient (*RAG-2*^{-/-}) blastocysts (14) to produce *LKLF*^{+/-}*RAG2*^{-/-} and *LKLF*^{-/-}*RAG2*^{-/-} chimeric mice. Because mature B and T cells cannot develop in the absence of RAG-2, all B and T cells in such chimeric mice are derived from the *LKLF*^{-/-} ES cells. Thus, the *RAG-2*^{-/-} chimera system provides a stringent test for the in-

Departments of Medicine and Pathology and The Committee on Genetics, University of Chicago, Chicago, IL 60637, USA.

*To whom correspondence should be addressed. E-mail: jleiden@medicine.bsd.uchicago.edu

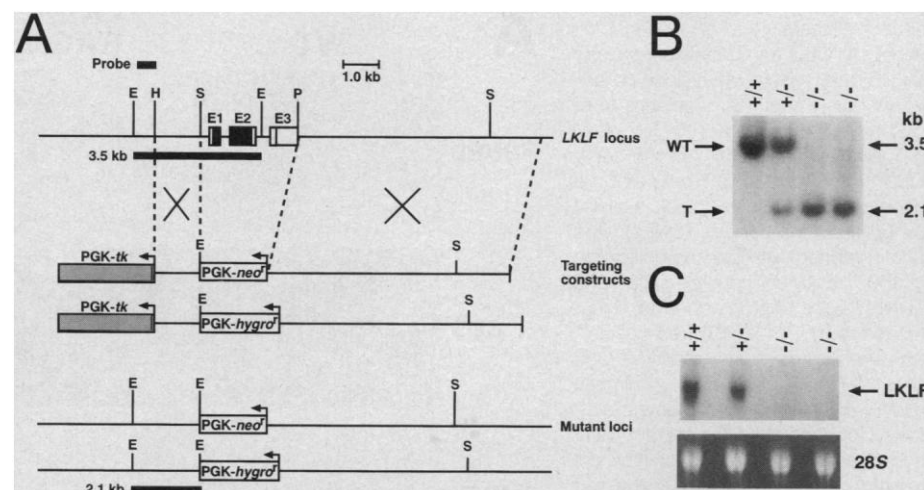
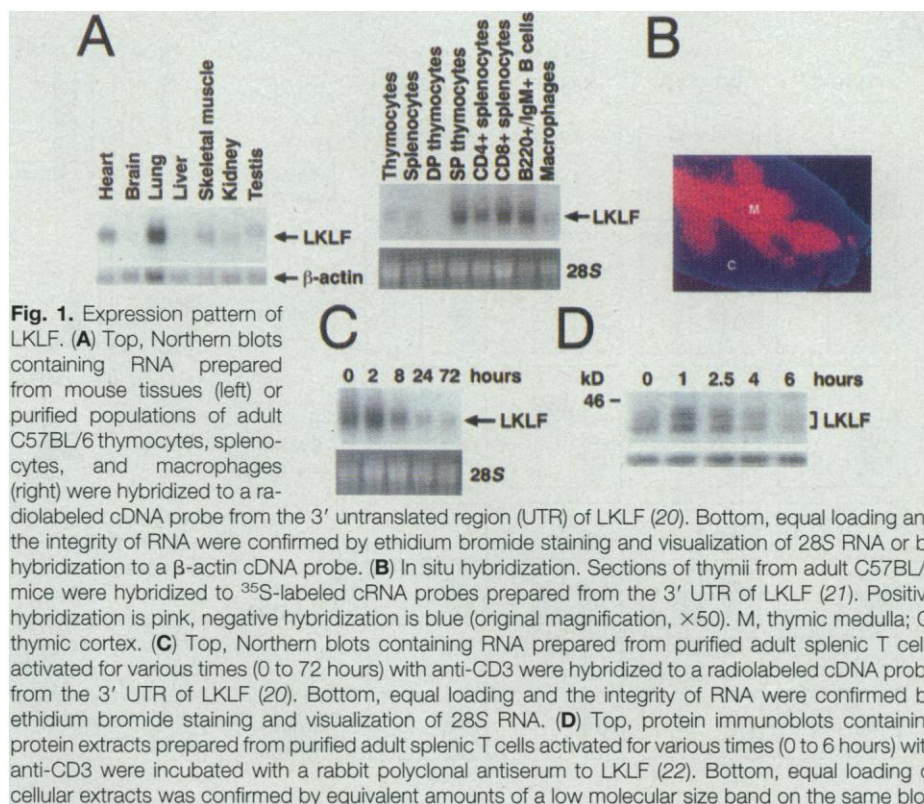
trinsic role of LKLF in B and T cell development and function in an environment of LKLF-expressing tissues (14).

In control experiments, injection of RAG-2^{-/-} blastocysts with LKLF^{+/-} ES cells fully rescued the defects in B and T cell development in the RAG-2^{-/-} animals (Fig. 3, A and B). LKLF^{+/-}RAG2^{-/-} mice contained normal populations of double-negative (DN) CD4⁻CD8⁻, DP, and SP thymocytes and peripheral T cells (Fig. 3A), normal populations of B220⁺IgM⁺ peripheral B cells (Fig. 3A), and normal concentrations of serum immunoglobulins (12). Consistent with these results, LKLF^{+/-} mice also displayed apparently normal lymphocyte development and function (12). In contrast, chimeric mice produced by injection of RAG-2^{-/-} blastocysts with LKLF^{-/-} ES cells displayed profound peripheral T cell defects. Total splenic and lymph node T cell numbers were reduced by more than 90% (Figs. 3, A and B) (12). The LKLF^{-/-}RAG2^{-/-} animals uniformly lacked circulating CD4⁺ and CD8⁺ T cells, as assessed by flow cytometry of peripheral blood leukocytes (Fig. 3A). In addition, both the CD4⁺ and CD8⁺ LKLF^{-/-} splenic and lymph node T cells displayed an abnormal cell surface phenotype (CD44^{hi}, CD69^{hi}, and L-selectin^{lo}) (Fig. 3C). This constellation of cell surface markers is characteristic of an activated as opposed to a quiescent peripheral SP T cell (3) and suggested that most LKLF^{-/-} peripheral T cells were spontaneously activated. However, these cells were not CD25⁺ (high-affinity interleukin-2 receptor) and were not proliferating as determined by propidium iodide fluorescence-activated cell sorting (FACS) analysis (12).

Several experiments were done to ensure that the peripheral T cell defects seen in the LKLF^{-/-}RAG2^{-/-} mice were not due to insufficient chimerism. Southern blot analysis of DNA isolated from multiple organs including heart, kidney, liver, skeletal muscle, and brain showed that all of the animals used in these studies were 60 to 90% chimeric (12). The SP T cell abnormalities described above were seen in all of the LKLF^{-/-}RAG2^{-/-} chimeric animals, which were produced by the injection of three independently derived LKLF^{-/-} ES cell clones, but in none of the LKLF^{+/-}RAG2^{-/-} chimeric animals, nor in any of more than 50 RAG-2^{-/-} chimeras produced with ES cells containing heterozygous or homozygous deletions of the Ets-1, Elf-1, or GATA-3 transcription factors (15). The same LKLF^{-/-}RAG2^{-/-} animals that lacked circulating T cells displayed normal numbers of mature (B220⁺IgM⁺) peripheral B cells in the

spleen, lymph nodes, and blood (Fig. 3, A and B) (12). Purified LKLF^{-/-} splenic B cells from these animals proliferated normally in response to treatment with lipopolysaccharide and to IgM cross-linking

and produced normal concentrations of serum immunoglobulins (12). Because it is more difficult to reconstitute the B cell than the T cell compartment in Rag-2^{-/-} chimeric animals (16), the finding of nor-



mal numbers of functionally intact B cells in the *LKLF^{-/-}RAG2^{-/-}* animals showed that the peripheral T cell defects seen in these animals were the result of LKLF

deficiency and were not due to insufficient lymphoid compartment chimerism. Although selective defects in the lymphoid cell lineages in the *RAG2^{-/-}* chimera

system are typically cell intrinsic, the high levels of chimerism of the *LKLF^{-/-}RAG2^{-/-}* animals used in these experiments did not allow us to exclude the

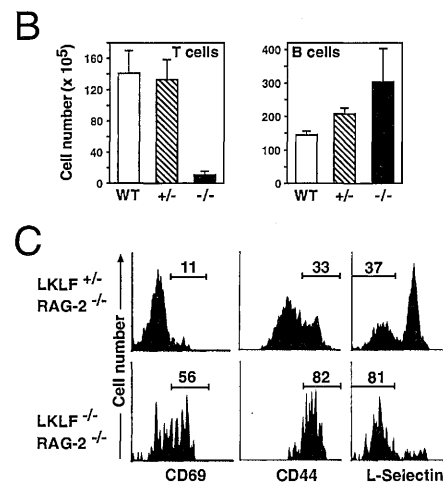
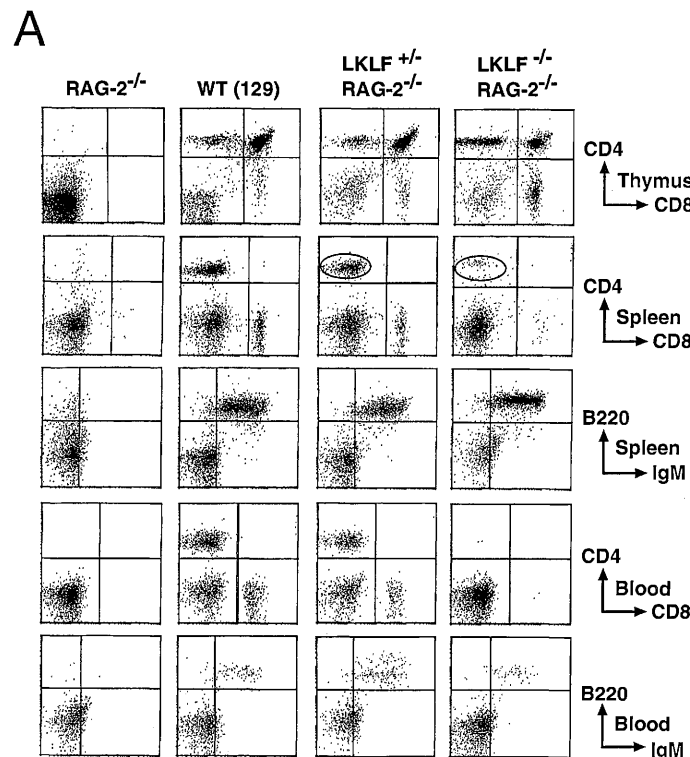
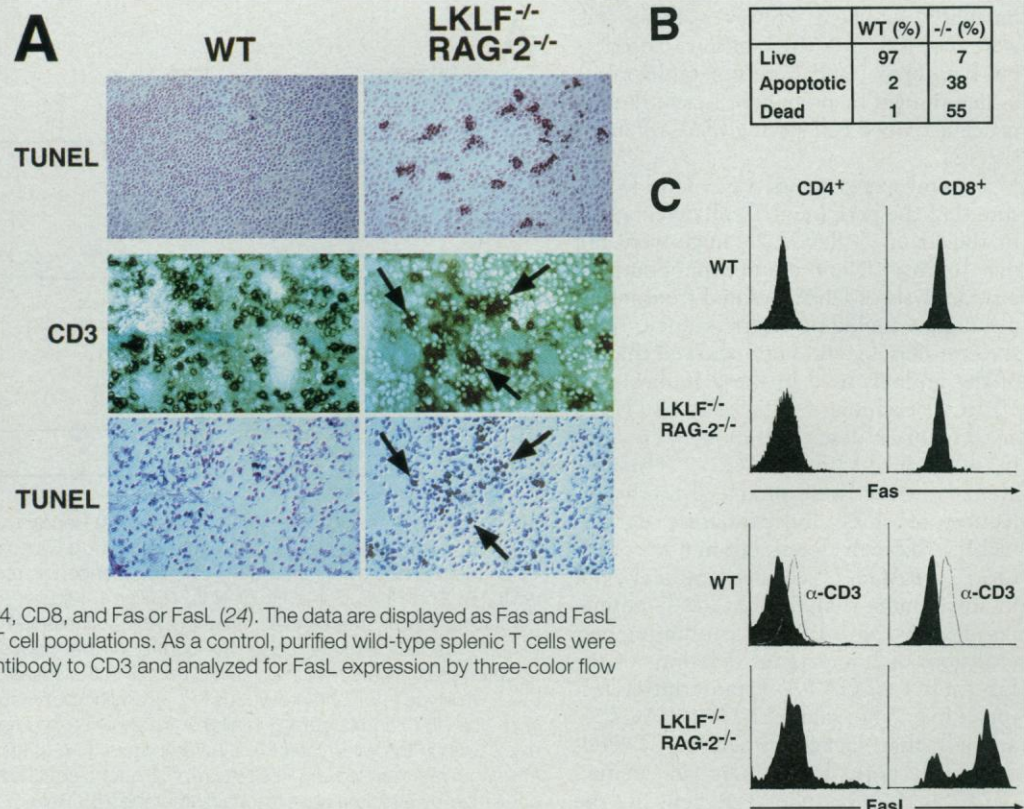


Fig. 3. Peripheral T cell defects in adult *LKLF^{-/-}RAG2^{-/-}* chimeric mice. (A) Thymocytes, splenocytes, and peripheral blood leukocytes were analyzed by two-color flow cytometry with antibodies to CD4 and CD8 or B220 and IgM. The results shown are representative of the analyses of at least five animals in each group (24). (B) T and B cell numbers in the spleens of wild-type (WT), heterozygous (+/-), and homozygous (-/-) chimeric animals. T cell numbers represent

the numbers of CD4⁺ and CD8⁺ SP splenocytes. B cell numbers represent the numbers of B220⁺IgM⁺ splenocytes. The results are shown as the mean \pm SEM for at least five animals in each group. (C) Flow cytometric analyses of splenocytes from *LKLF^{-/-}RAG2^{-/-}* chimeric mice. CD4⁺ SP splenocytes [see circled populations in (A)] were analyzed for expression of CD44, CD69, and L-selectin by three-color flow cytometric analyses (24). The results are representative of analyses performed on at least five animals in each group, and identical results were obtained in chimeras produced with three independently derived *LKLF^{-/-}* ES cell clones. Analyses of the CD8⁺ SP thymocytes from these animals yielded similar results (12).

Fig. 4. FasL-induced apoptosis of peripheral T cells in *LKLF^{-/-}RAG2^{-/-}* mice. (A) CD3 immunohistochemistry and TUNEL assays were done on adjacent tissue sections of spleens from wild-type (WT) and *LKLF^{-/-}RAG2^{-/-}* chimeric animals (25). Arrows show CD3⁺ (brown staining) T cells that are undergoing apoptosis (black staining by TUNEL). Top panels (TUNEL) were photographed at low magnification ($\times 150$), bottom panels (CD3 and TUNEL) were photographed at higher magnification ($\times 400$). (B) Freshly isolated splenocytes from wild-type and *LKLF^{-/-}RAG2^{-/-}* (-/-) chimeric mice were stained with 7-amino-actinomycin D and anti-CD4 and anti-CD8 and analyzed by three-color flow cytometry. Live, apoptotic, and dead cells were quantitated as described (7). (C) Freshly isolated splenocytes from wild-type and *LKLF^{-/-}RAG2^{-/-}* chimeric mice were analyzed by three-color flow cytometry for the expression of CD4, CD8, and Fas or FasL (24). The data are displayed as Fas and FasL expression on the SP (CD4⁺ and CD8⁺) T cell populations. As a control, purified wild-type splenic T cells were activated for 24 hours with monoclonal antibody to CD3 and analyzed for FasL expression by three-color flow cytometry (α -CD3; unshaded curves).



possibility that $LKLF^{-/-}$ cells of other lineages contributed to the observed T cell phenotype. To examine this possibility further, we analyzed $LKLF^{-/-}RAG2^{-/-}$ mice ranging in chimerism from 5 to 90%, each of which had fully reconstituted their B cell compartments. All of these animals displayed an identical T cell phenotype, suggesting that the observed T cell defects were cell intrinsic (12).

Several mechanisms might have been responsible for the severe peripheral T cell defects seen in the $LKLF^{-/-}RAG2^{-/-}$ mice. First, it was possible that LKLF was required for the production or survival of both of SP thymocytes. However, by flow cytometry, there was no evidence of a block in SP thymocyte production in the $LKLF^{-/-}RAG2^{-/-}$ animals (Fig. 3A). The $LKLF^{+/-}RAG2^{-/-}$ and $LKLF^{-/-}RAG2^{-/-}$ animals contained equivalent total numbers of thymocytes (12). Moreover, thymii from the $LKLF^{-/-}RAG2^{-/-}$ animals contained relatively increased numbers of SP cells and decreased numbers of DP cells as compared with the control $LKLF^{+/-}RAG2^{-/-}$ thymii (Fig. 3A). This reversal of the normal ratio of SP to DP thymocytes may have been primary or secondary. It is possible that the severely reduced numbers of peripheral SP T cells in the $LKLF^{-/-}RAG2^{-/-}$ mice fed back on the thymus to accelerate the differentiation of DP to SP cells or that there was a defect in the export of SP $LKLF^{-/-}$ thymocytes. It is also possible that there were defects in the survival or expansion of the DP population in these animals, although this seems less likely, because LKLF is not normally expressed in DP cells (Fig. 1A). Like the peripheral $LKLF^{-/-}$ T cells, both the $CD4^{+}$ and $CD8^{+}$ $LKLF^{-/-}$ SP thymocytes displayed a spontaneously activated cell surface phenotype ($CD44^{hi}$, $CD69^{hi}$, L-selectin^{lo}, $CD25^{-}$) yet were not proliferating as determined by propidium iodide FACS analysis (12). Finally, TdT-mediated dUTP nick end-labeling (TUNEL) assays failed to demonstrate evidence of increased thymocyte apoptosis in the $LKLF^{-/-}RAG2^{-/-}$ animals (12). Taken together, these experiments demonstrated that LKLF is not required for the production or survival of SP thymocytes, but instead, appears to play a critical role in programming the quiescent phenotype of SP thymocytes in vivo.

Because the $LKLF^{-/-}$ peripheral T cells displayed a spontaneously activated cell surface phenotype, and because there was no evidence of decreased production or survival of $LKLF^{-/-}$ SP thymocytes, we tested the hypothesis that increased apoptosis in the spleen and lymph nodes was responsible for the severely reduced num-

bers of peripheral T cells seen in the $LKLF^{-/-}RAG2^{-/-}$ mice. TUNEL assays demonstrated markedly increased numbers of apoptotic $CD3^{+}$ T cells in the white pulp of the spleen of the $LKLF^{-/-}RAG2^{-/-}$ mice (Fig. 4A). Consistent with this finding, 38% of freshly isolated $LKLF^{-/-}$ splenic T cells were apoptotic and 55% were dead (as compared with wild-type splenic T cells, 2% of which were apoptotic and 1% of which were dead) as determined by simultaneous staining with CD4, CD8, and 7-aminocoumarin D (Fig. 4B). In addition, purified $LKLF^{-/-}$ splenic T cells displayed a greater than fivefold increased rate of cell death as compared with wild-type T cells during in vitro culture for 14 hours in medium alone (12). Thus, the severe reduction in peripheral SP T cells seen in the $LKLF^{-/-}RAG2^{-/-}$ animals correlated with significantly increased rates of apoptosis of these cells both in vitro and in the peripheral lymphoid organs in vivo.

The finding that $LKLF^{-/-}$ SP T cells were highly susceptible to apoptosis suggested that LKLF might regulate the expression of genes such as Fas or Fas ligand (FasL) that are known to be involved in peripheral T cell apoptosis (4, 5). Resting peripheral T cells normally express the Fas receptor but fail to express FasL. TCR-mediated activation induces the expression of FasL on both $CD4^{+}$ and $CD8^{+}$ T cells. Engagement of Fas by FasL is thought to mediate the subsequent elimination of such activated T cell clones by apoptosis. Wild-type and $LKLF^{-/-}$ $CD4^{+}$ and $CD8^{+}$ splenic T cells expressed equivalent amounts of Fas (Fig. 4C). In contrast, both $CD4^{+}$ and $CD8^{+}$ $LKLF^{-/-}$ splenic T cells displayed significantly increased amounts of cell surface FasL as assayed by FACS. Amounts of FasL on the $LKLF^{-/-}$ SP T cells were equivalent to (on the $CD4^{+}$ cells) or higher than (on the $CD8^{+}$ cells) those observed after TCR-mediated activation of wild-type splenic T cells (Fig. 4C). Taken together, these results were consistent with a model in which $LKLF^{-/-}$ T cells undergo spontaneous activation, express FasL, and die from subsequent Fas-mediated apoptosis in the peripheral lymphoid organs.

Our findings suggest that T cell quiescence and survival, like T cell activation, are programmed by specific transcriptional regulatory pathways and identify LKLF as an important regulator of one such pathway. The evolution of this pathway may reflect the need to maintain a large pool of quiescent peripheral T cell clones while preventing spontaneous T cell activation and the concomitant risk of autoimmune disease. The identification of this pathway

suggests future studies aimed at understanding both the potential targets of LKLF and its developmental and post-translational regulation. Preliminary experiments suggest that LKLF degradation is mediated by a protein kinase C-dependent pathway and that degradation is preceded by alterations in the electrophoretic mobility of the protein, suggesting that phosphorylation or ubiquitination might regulate the stability of LKLF in T cells (12). Our finding of spontaneous FasL expression on the $LKLF^{-/-}$ SP T cells suggests that LKLF might negatively regulate the FasL promoter. Understanding how LKLF is regulated and what it is regulating should help to elucidate the molecular basis of T cell quiescence and may also be relevant for understanding and modulating pathophysiological T cell activation that contributes to the pathogenesis of human autoimmune disease.

REFERENCES AND NOTES

1. C. A. Janeway and K. Bottomly, *Cell* **76**, 275 (1994); I. L. Weissman, *ibid.*, p. 207; J. M. Green and C. B. Thompson, *Immunol. Res.* **13**, 234 (1994).
2. J. D. Fraser, D. Straus, A. Weiss, *Immunol. Today* **14**, 357 (1994); A. Weiss and D. R. Littman, *Cell* **76**, 263 (1994); G. R. Crabtree, *Science* **243**, 355 (1989).
3. A. Bendelac, P. Matzinger, R. A. Seder, W. E. Paul, R. H. Schwartz, *J. Exp. Med.* **175**, 731 (1992); F. Ramsdell, M. Jenkins, Q. Dinh, B. J. Fowlkes, *J. Immunol.* **147**, 1779 (1991); R. C. Budd *et al.*, *ibid.* **138**, 3120 (1987); W. M. Yokoyama *et al.*, *ibid.* **141**, 369 (1988); T. M. Jung, W. M. Gallatin, I. L. Weissman, M. O. Dailey, *ibid.*, p. 4110.
4. L. H. Boise, A. R. Gottschalk, J. Quintans, C. B. Thompson, *Curr. Topics Microbiol. Immunol.* **200**, 107 (1995); J. H. Russell, *Curr. Opin. Immunol.* **7**, 382 (1995).
5. A. K. Abbas, *Cell* **84**, 655 (1996); L. Van Parijs, A. Ibraghimov, A. K. Abbas, *Immunity* **4**, 321 (1996).
6. P. A. Baeuerle and D. Baltimore, *Cell* **87**, 13 (1996); J. P. Northrop *et al.*, *Nature* **369**, 497 (1994); P. G. McCaffrey *et al.*, *Science* **362**, 750 (1993); A. R. Farina, T. Davis-Smyth, K. Gardner, D. Levens, *J. Biol. Chem.* **268**, 26466 (1993); E. S. Masuda *et al.*, *Mol. Cell. Biol.* **13**, 7399 (1993); J. M. Leiden and C. B. Thompson, *Curr. Opin. Immunol.* **6**, 231 (1994); J. M. Leiden, *Annu. Rev. Immunol.* **11**, 539 (1993).
7. K. Barton *et al.*, *Nature* **379**, 81 (1996).
8. H. C. Clevers and R. Grosschedl, *Immunol. Today* **17**, 336 (1996).
9. I. J. Miller and J. J. Bleker, *Mol. Cell. Biol.* **13**, 2776 (1993); J. J. Bleker, C. M. Southwood, *ibid.* **15**, 852 (1995); M. Merika and S. H. Orkin, *ibid.*, p. 2437; D. Donze, T. M. Townes, J. J. Bleker, *J. Biol. Chem.* **270**, 1955 (1995); A. C. Perkins, A. H. Sharpe, S. H. Orkin, *Nature* **375**, 318 (1995); B. Nuez, D. Michalovich, A. Bygrave, R. Ploemacher, F. Grosveld, *ibid.*, p. 316; M. Wijgerde *et al.*, *Genes Dev.* **10**, 2894 (1996).
10. A radiolabeled 78-base pair (bp) degenerate oligonucleotide, 5'-GTGKCKBKTSAGYTSGTCTGAC-CGMGMIRAACCKYCWYSYRCAGYCBTYSMASK-NRCASKSRTANGGYTTCTCWCNGT-3', derived from the zinc finger region of the murine EKLF cDNA was hybridized to an embryonic day 12.5 mouse cDNA library (Stratagene) in 6× standard saline citrate (SSC) (1× SSC = 0.15 M NaCl, 0.015 M sodium citrate, pH = 7.0), 3× Denhardt's solution, 2 mM EDTA, 0.5% SDS, and salmon sperm DNA (100 µg/ml) at 65°C overnight. The filters were washed in

- 6X SSC, 0.1% SDS at 65°C for 1 hour and autoradiographed. Positive clones were purified to homogeneity and subjected to dideoxy sequence analysis. LKLF genomic clones were isolated from a 129sv genomic library (Stratagene) by hybridization to the LKLF cDNA and characterized by restriction enzyme and DNA sequence analyses.
11. M. Crossley *et al.*, *Mol. Cell. Biol.* **16**, 1695 (1996); J. M. Shields, R. J. Christy, V. W. Yang, *J. Biol. Chem.* **271**, 20009 (1996); K. P. Anderson, C. B. Kern, S. C. Crable, J. B. Lingrel, *Mol. Cell. Biol.* **15**, 5957 (1995).
 12. C. T. Kuo, M. Vasselits, J. M. Leiden, unpublished data.
 13. C. T. Kuo, M. Vasselits, K. Barton, C. Clendenin, J. M. Leiden, in preparation.
 14. J. Chen, R. Lansford, V. Stewart, F. Young, F. W. Alt, *Proc. Natl. Acad. Sci. U.S.A.* **90**, 4528 (1993).
 15. N. Muthusamy, K. Barton, J. M. Leiden, *Nature* **377**, 639 (1995); C. N. Ting, M. C. Olson, K. P. Barton, J. M. Leiden, *ibid.* **384**, 474 (1996); K. Barton, N. Muthusamy, J. M. Leiden, unpublished data.
 16. J. Chen and F. W. Alt, in *Transgenics and Targeted Mutagenesis*, H. Bluthmann and P. Ohashi, Eds. (Academic Press, San Diego, CA, 1994), pp. 35–49; J. Chen, Y. Shinkai, F. Young, F. W. Alt, *Curr. Opin. Immunol.* **6**, 313 (1994).
 17. E. E. Morrisey, H. S. Ip, M. M. Lu, M. S. Parmacek, *Dev. Biol.* **177**, 309 (1996).
 18. V. L. Tybulewicz, C. E. Crawford, P. K. Jackson, R. T. Bronson, R. C. Mulligan, *Cell* **65**, 1153 (1991).
 19. Y. Gavrieli, Y. Sherman, S. A. Ben-Sasson, *J. Cell Biol.* **119**, 493 (1992); D. A. Baunoch *et al.*, *Int. J. Oncol.* **8**, 895 (1996).
 20. Purified DP and SP thymocytes and splenocytes were obtained by flow cytometric cell sorting on a FACStarPLUS (Becton Dickinson) after staining with monoclonal antibody (mAb) to CD4 (RM4-5) and mAb to CD8 (53-6.7) (PharMingen). These preparations were more than 95% pure as determined by repeat flow cytometry. CD4⁺ and CD8⁺ splenocytes were obtained by purification on a commercially available column according to the manufacturer's instructions (R&D Systems). Splenic T cells (4×10^6 cells/ml) were activated by treatment for 2 to 72 hours at 37°C with immobilized mAb to CD3 (145.2C11) (16 µg/ml). RNA was isolated with TRIzol reagent (GIBCO-BRL) and subjected to Northern blot analysis.
 21. In situ hybridizations were done as described (17). Dark-field photomicrographs were obtained with a Zeiss Axioskop (original magnification, $\times 50$).
 22. Purified and activated SP T cells were homogenized in SDS-polyacrylamide gel electrophoresis (PAGE) loading buffer, resolved by SDS-PAGE, transferred to nitrocellulose membranes, and subjected to protein immunoblotting with a rabbit polyclonal antiserum to LKLF. To generate this antiserum, we cloned nucleotides 1 to 484 from the LKLF cDNA in-frame downstream of glutathione-S-transferase (GST) in the bacterial expression vector pGEX-4T-3 (Pharmacia). The GST fusion protein was expressed in bacteria and purified on glutathione beads according to manufacturer's protocol. Rabbits were immunized with the purified GST fusion protein by Pocono Rabbit Farm and Laboratory (Canadensis, PA).
 23. The *neo^r* targeting vector was generated by inserting a 7.1-kb Pac I–Not I genomic fragment of the murine *LKLF* locus into the Xho I–Not I site of pPNT (18), followed by ligation of a 1.4-kb Hind III–Sal I genomic fragment located 5' of the *LKLF* gene into the Eco RI site of pPNT. The *hygro^r* targeting vector was generated by replacing the PGK-*neo^r* cassette in the *neo^r* LKLF targeting construct with a PGK-*hygro^r* cassette. The resulting targeting constructs were linearized with Not I before electroporation into CCE ES cells. *Neo^r* transfectants were selected by growth in G418 (200 mg/ml) and gancyclovir (1 mM). DNA samples from ES cell clones were characterized by Southern blot analysis by using Eco RI digestion and a radiolabeled 0.5-kb Hind III–Msc I genomic probe (probe, Fig. 2A). LKLF^{-/-} ES cells were generated by electroporating LKLF^{+/-} *neo^r* ES cells with the *hygro^r* targeting vector. Transfectants were selected by growth in hygromycin B (150 mg/ml) and gancyclovir (1 mM), and DNA samples from ES cell clones were characterized by Southern blot analysis as described above.
 24. Single-cell suspensions of lymphocytes (0.5×10^6 to 1.0×10^6 cells) were washed in phosphate-buffered saline (PBS) with 0.1% sodium azide and stained in PBS and 0.1% bovine serum albumin for 30 min on ice with phycoerythrin (PE)-, fluorescein isothiocyanate (FITC)-, and Cy-Chrome-conjugated antibodies. The antibodies used in these experiments are the following: anti-CD4 (RM4-5), anti-CD8 (53-6.7), anti-CD45RB220 (RA3-6B2), anti-IgM (II/41), anti-CD44 (IM7), anti-L-selectin (MEL-14), anti-CD69 (H1.2F3), anti-CD25 (3C7), anti-CD28 (37.5.1), anti-Fas (Jo2), and anti-FasL (NOK-1) (PharMingen). Flow cytometric analyses were performed on a FACScan (Becton Dickinson). In two-color flow cytometric analyses, gating for viable cells was performed with propidium iodide exclusion. Each plot represents the analysis of more than 10^4 events with WinMDI 2.0.7 software.
 25. TUNEL assays and CD3 immunohistochemistry were performed on frozen sections according to procedures previously described (19). Photomicrographs were obtained with a Zeiss Axioskop. Splenic T cell viabilities were assayed by simultaneous staining with 7-amino-actinomycin D and PE-conjugated mAb to CD4 and FITC-conjugated mAb to CD8 (Pharmingen) (7).
 26. We thank C. Clendenin, and K. Sigrist for technical assistance with the preparation of chimeric mice; M. Lu and D. Baunoch for technical assistance with histological analyses; P. Lawrey and L. Gottschalk for help with the preparation of the manuscript and illustrations; M. Parmacek, J. Bluestone, E. McNally, and M. C. Simon for helpful discussions; R. Anandappa for technical assistance with LKLF antibody generation; and J. Auger for technical assistance with FACS analysis. Supported in part by a grant to J.M.L. from NIH (A129637) and by the Cancer Center of the University of Chicago.

6 May 1997; accepted 1 August 1997

Aggregation of Huntingtin in Neuronal Intranuclear Inclusions and Dystrophic Neurites in Brain

Marian DiFiglia,* Ellen Sapp, Kathryn O. Chase, Stephen W. Davies, Gillian P. Bates, J. P. Vonsattel, Neil Aronin

The cause of neurodegeneration in Huntington's disease (HD) is unknown. Patients with HD have an expanded NH₂-terminal polyglutamine region in huntingtin. An NH₂-terminal fragment of mutant huntingtin was localized to neuronal intranuclear inclusions (NIIs) and dystrophic neurites (DNs) in the HD cortex and striatum, which are affected in HD, and polyglutamine length influenced the extent of huntingtin accumulation in these structures. Ubiquitin was also found in NIIs and DN, which suggests that abnormal huntingtin is targeted for proteolysis but is resistant to removal. The aggregation of mutant huntingtin may be part of the pathogenic mechanism in HD.

The pathology of HD is marked by a preferential loss of neurons in the striatum and cortex (1). The genetic mutation is an unstable and expanded CAG repeat in the gene that encodes huntingtin (2). Larger polyglutamine expansions in huntingtin are associated with earlier onset and increased severity of the disease (3). Because mutant huntingtin is expressed throughout the brain in HD (4), its involvement in selective cell death in the striatum and cortex is unclear.

Two pathogenic processes have been suggested as the basis for neurodegenera-

tion in HD. One process involves interaction of mutant huntingtin with other proteins to produce a change of function. Alternatively, mutant huntingtin might homodimerize (5) or heterodimerize (6) to build large, poorly soluble protein aggregates. Proteins that interact more avidly with NH₂-terminal products of mutant huntingtin than with wild-type have been identified but are found throughout the brain with no preferential distribution in those regions affected in HD (7). Analysis of the HD brain (8) with an antiserum that recognizes an internal region of huntingtin in wild-type and mutant proteins showed that the subcellular distribution of huntingtin in the cytoplasm of neurons was abnormal, but the contribution of mutant huntingtin to these changes was unclear. In a recent study of HD transgenic mice expressing an NH₂-terminal mutant huntingtin fragment with 115 to 156 glutamine repeats, we found that intraneuronal nuclear inclusions reactive to NH₂-terminal antiserum to huntingtin devel-

M. DiFiglia, E. Sapp, J. P. Vonsattel, Department of Neurology, Massachusetts General Hospital, Boston, MA 02114, USA.

S. W. Davies, Department of Anatomy and Developmental Biology, University College London, Gower Street, London WC1E, 6BT, UK.

G. P. Bates, Division of Medical and Molecular Genetics, UMDS Guy's Hospital, London SE1 7E H, UK.

K. O. Chase, N. Aronin, Departments of Medicine and Cell Biology, University of Massachusetts Medical Center, Worcester, MA 01655, USA.

*To whom correspondence should be addressed.